A Market Equilibrium Model for Electricity, Gas and District Heating Operations

Xi, Yufei; Zeng, Qing; Chen, Zhe; Lund, Henrik; Conejo, Antonio J.

Published in:
Energy

DOI (link to publication from Publisher):
10.1016/j.energy.2020.117934

Publication date:
2020

Document Version
Accepted author manuscript, peer reviewed version

A Market Equilibrium Model for Electricity, Gas and District Heating Operations

Yufei Xi [a], Qing Zeng [b]*, Zhe Chen [a], Henrik Lund [c], Antonio J. Conejo [d]

[a] *Department of Energy Technology, Aalborg University, 9220, Aalborg, Denmark*

[b] * *Sichuan Energy Internet Research Institute, Tsinghua University, 610000, Chengdu, Sichuan, China*

[c] *Department of Development and Planning, Aalborg University, 9000 Aalborg, Denmark*

[d] *Department of Electrical and Computer Engineering, and Department of Integrated System Engineering, The Ohio State University, 43210, Columbus, Ohio, USA*

*zengqing1027@hotmail.com

***Abstract*:** With increasing penetration of renewable energy, multi-energy systems constitute an effective mechanism to optimize energy distribution and improve social welfare. However, a centralized operation of the multi-energy system might not be appropriate under the existing energy markets. Therefore, this paper proposes an equilibrium model for improving the operation of the electricity, gas and district heating subsystems of a district or urban area. The proposed model allows each energy subsystem to pursue its own objective (i.e., maximum social welfare), while considering the interconnection with other subsystems. More specifically, this model represents the behavior of each subsystem and reflects the interactions of the multi-energy system in a practical way. This equilibrium problem is formulated as a nonlinear complementarity problem. An illustrative case study is analyzed to show the relevance of the proposed approach.

***Index Terms*:** Electric power system; natural gas system; district heating system; multi-energy system; equilibrium problem.

Nomenclature

Scripts, sets and indices

PL, GL, HL	Power load, gas load, heat load of consumers
CFP, WF	Coal-fired power plant, wind farm
S, P2G, GC	Gas source, power to gas, gas compressor

CHP, HP	Combined heat and power, heat pump
LP, GS, HS	Linpack, gas storage, heat storage
Ω	Set of energy units
Λ	Set of nodes or buses
e, *g*, *h*	Index of nodes in the power, gas, heat network
i, *j*, *p*, *k*, *f*, *s*	Index of energy units
m, *n*	Index of nodes or pipelines
t	Index of time

Parameters

D_{mn}, l_{mn}	The diameter, length of pipeline *m*-*n* [m]
k_{mn}	Heat transfer coefficient of pipeline *m*-*n* [MW/(m^2°C)]
T_s	Suction temperature of compressor [°C]
η^{GC}	Compression efficiency
E^{GC}	Parasitic efficiency of compressor
c_k	Specific heat ratio for natural gas
Z_a	Average compressibility factor

Acronyms

MES	Multi-energy system
GPG	Gas-fired power generator
EPS	Electric power system
NGS	Natural gas system
DHS	District heating system
MPEC	Mathematical program with equilibrium constraints
EPEC	Equilibrium problem with equilibrium constraints

GNEP Generalized Nash Equilibrium Problem

1. INTRODUCTION

Coordinating the operation of different energy systems such as electricity, gas, heating, cooling and transport as an integrated multi-energy system (MES) provides opportunities to improve the economic and environmental performance of energy utilization [1]-[5]. Meanwhile, the increasing use of energy conversion technologies (e.g., gas-fired power generators (GPGs), heat pumps (HPs), combined heat and power (CHP) units, and power-to-gas (P2G) stations) increases the interdependence among the electric power system (EPS), the natural gas system (NGS) and the district heating system (DHS). Therefore, the joint operation of EPS, NGS and DHS is an important research topic, considered in a number of recent studies.

The research on coordination of gas and power systems mainly pertains to a national or regional level. This is because the NGS and the EPS interact for bulk energy transmission across a country, even a continent. A unified energy flow model is developed to describe the steady-state operation of integrated gas and power systems in [6], while [7] formulates a dynamic optimal energy flow model for integrated gas and power systems by considering the different response times of both systems. With the increasing deployment of renewables, many coordination studies focus on the flexibility of gas-power systems to accommodate renewable energy. Reference [8] presents a stochastic model to study the role of demand response in the operation of power systems considering natural gas transmission constraints. Reference [9] presents a two-stage stochastic unit commitment model to analyze the scheduling of electricity production units under natural gas supply uncertainty. Reference [10] proposes a robust optimization approach to deal with the scheduling of quick-start units with natural gas transmission constraints. Additionally, the above studies show that the coordination of electricity and natural gas infrastructure facilitates the integration of renewable energy.

The research on coordination of heat and power systems mainly focuses on the urban or district level, where DHSs have been adopted to supply heat with high efficiency. Most efforts in this area pertain to the

development of algorithm. Reference [11] compares integrated and decomposed solution techniques in analyzing the operation of combined power and heat networks. It shows that the integrated method requires less computational effort than the decomposed one. Reference [12] proposes a decomposition-coordination algorithm to solve the optimization problem of operating electricity and heating systems. The results indicate that the coordinated optimization has significant benefits for reducing operational cost and energy losses. Some other works focus specifically on integrated heat and power systems. A heat and power combined dispatch model is presented in [13] and a transmission-constrained unit commitment model is presented in [14]. These works conclude that exploiting heat storage capacity provides a cost-saving way to increase the flexibility of the EPS to accommodate high penetration of wind power.

A number of research efforts have been devoted to the optimal operation of MESs. However, all these studies assume that there is a central entity, which jointly operates all the energy subsystems (including gas, power and heating facilities). This paper proposes a multi-energy equilibrium model where each subsystem acts as an independent agent that pursues its own profit maximization. To better illustrate energy trading and market outcomes in these coupled energy subsystems, several mathematical structures are used for analyzing the behaviors of the participants in the energy markets, including equilibrium problems, mathematical programs with equilibrium constraints (MPECs) and equilibrium problems with equilibrium constraints (EPECs) [15]. Once a market reaches an equilibrium, no market participant can benefit from changing its strategy while the other participants keep their strategies unchanged [16]. The concepts and models of equilibrium for electricity markets are reported in [17] and [18]. An oligopolistic market model for analyzing electricity markets is presented in [19], in which each generating firm is modelled as a MPEC that submits bids to a central system operator to maximize its profit. For an EPEC, equilibria can be characterized by jointly solving the Karush-Kuhn-Tucker (KKT) conditions of all the problems involved [20]. A stochastic EPEC to model the multi-agent strategic-offering in a pool-based electricity market with stochastic demands is proposed in [21]. An EPEC can be solved by diagonalization as described in [22]. It is important to note that the application of these equilibrium models is mostly limited to electricity systems and markets.

In most research works for MES, a centralized optimization problem is formulated to pursue a single objective (its overall profit) while meeting all network constraints based on the assumption of perfect coordination among the operators of different energy systems. However, the operators providing the heat, gas and electricity act generally independently or with limited coordination (regarding interexchange of information). The proposed model explicitly allows operators to pursue their own objectives through an equilibrium model for multi-energy markets that reflects the interactions among the multiple operators in the MES. Two models are developed to describe the joint operation of the MES in a district or urban area, which are formulated as a centralized optimization problem and as an equilibrium problem. The contributions of this paper are summarized as follows:

1. A centralized operation model is developed for a MES controlled by one central entity that jointly operates the EPS, NGS and DHS to maximize social welfare. This model is a single nonlinear optimization problem that is solved by using the solver IPOPT.

2. A multi-energy equilibrium model is developed for a MES, where the operator of each subsystem not only acts as an energy player to maximize its own social welfare from trading in the energy market, but also considers the interconnection with the other subsystems. This model is a nonlinear complementarity equilibrium problem that is solved by using the solver PATH [23].

3. A detailed comparison of the centralized operation model and the multi-energy equilibrium model is carried out.

4. Market prices are investigated to further explore the interactions among the different subsystems.

5. The proposed model is used to better understand the effect of different wind power production levels on the market behavior and energy exchange.

The remainder of the paper is organized as follows. Section II presents the models of the electricity, gas and heat subsystems that constitute the multi-energy market model. For the sake of comparison, a centralized operation model is formulated to represent the joint scheduling of the electricity, gas and heat subsystems. Section III presents the solution methodology proposed, and Section IV analyzes case studies. Finally,

Section V gives conclusions.

2. MODEL FORMULATION

2.1 The structure of the multi-energy market model

A multi-energy market model including three subsystems is considered below. The roles and interactions of the subsystem operators are shown in Fig. 1. Each subsystem (NGS, DHS and EPS) has its own operator to control the energy allocation and market trading.

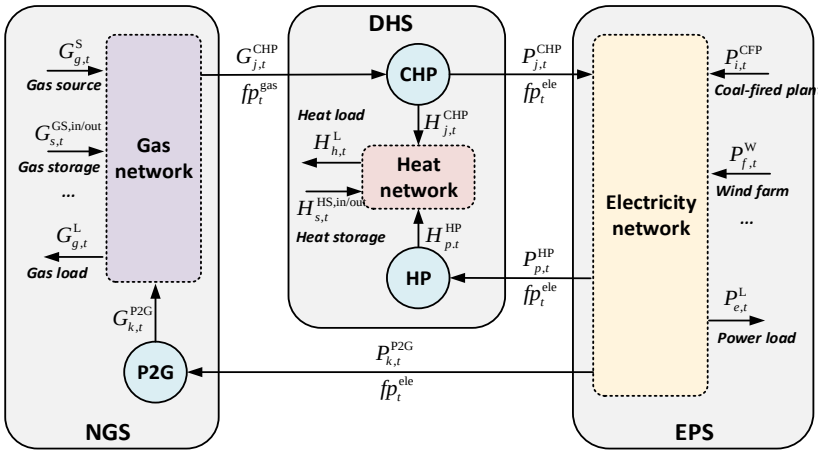

Fig. 1. The structure of the multi-energy market model

The NGS has five components including gas sources, gas storages, gas loads, P2G units and the gas network. P2G units are controlled by the NGS operator and convert electricity to gas. The EPS includes coal-fired power (CFP) units, wind farms, power loads and the electricity network. The DHS includes CHP units, HPs, heat storages, heat loads and the heat network. The CHP units are controlled by the DHS operator and generate electricity and heat simultaneously by consuming natural gas. It is worth mentioning that the power generation of any CHP unit is determined by the heat generation. We note that, if the heat would be supplied solely by the gas-fired CHP units, the heat supply would be monopolized by the NGS. Thus, in order to prevent this and analyze more relevant cases, the DHS also uses HPs to supply heat.

In the multi-energy market, the NGS acts as a prosumer, which can buy electricity from the EPS to run P2G units and sell gas later on to the EPS or the DHS in the pursuit of a profit. The NGS acts as a pure provider if P2G units are not considered in the MES. The EPS also acts as a prosumer. On the one hand, it

buys electricity from CHP plants. On the other hand, it may sell electricity to run the HPs for the DHS. When there is a surplus of wind power, it may sell electricity to run the P2G units. To prevent the NGS to control the power market, a number of power sources are available including CFP units, wind power units and others to meet the electricity demand. The DHS acts as a prosumer as well. It can buy gas from the NGS or electricity from the EPS to supply heat. Additionally, the DHS sells electricity from CHP units to the EPS. It is important to note that there are decision variables ($G_{j,t}^{\mathrm{CHP}}$, $P_{j,t}^{\mathrm{CHP}}$, $P_{p,t}^{\mathrm{HP}}$, $P_{k,t}^{\mathrm{P2G}}$) common to the different subsystems, which describe the energy trading among the different operators. Besides, the actions of any operator will influence the actions of the other operators, and the market clearing conditions enforce that the energy supply in each subsystem equals the energy demand in the corresponding subsystem.

2.2 Equilibrium model

A typical centralized model entails a cooperative process in which all the subsystems agree on a single optimization objective pursued by one central system operator. Such an optimization requires perfect information interexchange among all the subsystems. However, in fact, the operators of the heat, gas and electricity systems generally operate independently or have limited coordination and information interchange. Hence, the centralized optimization scheme might not be adequate to model a MES and to characterize multi-energy transaction in markets.

In this section, an equilibrium model is developed based on the Nash Equilibrium concept [24]. In contrast to a centralized model, a Nash Equilibrium model is a non-cooperative game, where the operator of each subsystem pursues its own benefit until an equilibrium is achieved [25]. Thus, the equilibrium model preserves the independence of each subsystem and allows modeling the market interactions of the subsystems from different perspectives.

In this multi-energy market, each operator maximizes its profit taking into account its own constraints. The combination of the optimization problems of the three operators constitutes an equilibrium problem. The ‘own constraints’ are the operational constraints of each subsystem. The optimal operation models for the power, gas and heat subsystems are formulated individually. In each operating model, the objective function

is formulated as social welfare. The social welfare is defined as the producers' surplus plus the consumers' surplus. For simplicity, we consider the fuel cost as the operational cost [7]. In this paper, all objective functions represent negative social welfare. Thus, objective functions are minimized.

1) Optimal operation of the EPS

In the multi-energy model, the operation of the EPS aims at maximizing its social welfare, which represents the difference between the total revenue and the total operational cost. The negative social welfare is minimized below.

$$\begin{aligned} f_{\mathrm{E}}(x) = \min_{\boldsymbol{x}^{\mathrm{EPS}}} \sum_{t\in T} \Bigg\{ & \sum_{i\in\Omega^{\mathrm{CFP}}} C_i^{\mathrm{CFP}} P_{i,t}^{\mathrm{CFP}} + \sum_{j\in\Omega^{\mathrm{CHP}}} fp_t^{\mathrm{ele}} P_{j,t}^{\mathrm{CHP}} + \sum_{e\in\Omega^{\mathrm{PL}}} \sigma_{e,t}^{\mathrm{UE}} P_{e,t}^{\mathrm{UE}} \\ & - \sum_{p\in\Omega^{\mathrm{HP}}} fp_t^{\mathrm{ele}} P_{p,t}^{\mathrm{HP}} - \sum_{k\in\Omega^{\mathrm{P2G}}} fp_t^{\mathrm{ele}} P_{k,t}^{\mathrm{P2G}} - \sum_{e\in\Omega^{\mathrm{PL}}} u_{e,t}^{\mathrm{PL}} P_{e,t}^{\mathrm{L}} \Bigg\} \end{aligned} \tag{1}$$

where T is the set of time periods and $\boldsymbol{x}^{\mathrm{EPS}}$ identifies the set of decision variables of the EPS. Constants $C_i^{\mathrm{CFP}}$and $\sigma_{e,t}^{\mathrm{UE}}$ are the marginal cost of power production from CFP unit i and the penalty cost of unserved electrical energy, respectively. Variable fp_t^{ele} represents the hourly electricity price. Variable $P_{e,t}^{\mathrm{UE}}$ and $P_{e,t}^{\mathrm{L}}$ are the unserved load and the hourly power load at bus e, respectively. Variables $P_{i,t}^{\mathrm{CFP}}$ and $P_{j,t}^{\mathrm{CHP}}$ represent the hourly electricity generation of CFP unit i and CHP unit j, respectively. Variables $P_{p,t}^{\mathrm{HP}}$ and $P_{k,t}^{\mathrm{P2G}}$ represent the hourly electricity consumption of HP p and P2G unit k, respectively. Thus, the objective function in the EPS optimization includes six components: the operational cost of CFP units to produce electricity, the cost of buying electricity from CHP units, the penalty cost pertaining to unserved loads, the revenue from selling electricity to HPs, the revenue from selling electricity to P2G units and the total utility for electricity consumers, which is calculated by multiplying the amount of power loads and the marginal utility of electricity consumption ($u_{e,t}^{\mathrm{PL}}$). Here, the marginal utility of electricity consumption is assumed to be constant.

For the electricity network, a DC power flow representation is adopted [21].

$$\begin{aligned}&\sum_{j\in\Omega^{\mathrm{CHP}}}P_{j,t}^{\mathrm{CHP}}+\sum_{i\in\Omega^{\mathrm{CFP}}}P_{i,t}^{\mathrm{CFP}}+\sum_{f\in\Omega^{\mathrm{WF}}}P_{f,t}^{\mathrm{W}}\\&-\sum_{k\in\Omega^{\mathrm{P2G}}}P_{k,t}^{\mathrm{P2G},}-\sum_{p\in\Omega^{\mathrm{HP}}}P_{p,t}^{\mathrm{HP}}-\sum_{e\in\Omega^{\mathrm{PL}}}\left(P_{e,t}^{\mathrm{L}}-P_{e,t}^{\mathrm{UE}}\right)\\&=\sum_{n\in\Lambda_m}B_{mn}\left(\delta_{m,t}-\delta_{n,t}\right),\qquad\forall t\in T,\forall m\in\Lambda^{\mathrm{EPS}}\end{aligned}\tag{2}$$

Where variable $P_{f,t}^{\mathrm{W}}$ is the hourly on-grid wind power from wind farm *f*. The active power flow through transmission line *m*-*n* is the product of the line susceptance (B_{mn}) and the difference between phase angles at bus *m* ($\delta_{m,t}$) and bus *n* ($\delta_{n,t}$). The power flow of each transmission line is bounded by its transmission capacity (P_{mn}^{TL}).

$$\left|B_{mn}\left(\delta_{m,t}-\delta_{n,t}\right)\right|\le P_{mn}^{\mathrm{TL}},\quad\forall m,n\in\Lambda^{\mathrm{EPS}},\forall t\in T\tag{3}$$

For each CFP/CHP unit, the electricity production and production change should be within its operational limits.

$$\begin{cases}P_i^{\mathrm{CFP,min}}\le P_{i,t}^{\mathrm{CFP}}\le P_i^{\mathrm{CFP,max}},&\forall i\in\Omega^{\mathrm{CFP}},\forall t\in T\\P_j^{\mathrm{CHP,min}}\le P_{j,t}^{\mathrm{CHP}}\le P_j^{\mathrm{CHP,max}},&\forall j\in\Omega^{\mathrm{CHP}},\forall t\in T\end{cases}\tag{3}$$

$$\begin{cases}\left|P_{i,t}^{\mathrm{CFP}}-P_{i,t-1}^{\mathrm{CFP}}\right|\le\Delta P_i^{\mathrm{CFP}},&\forall i\in\Omega^{\mathrm{CFP}},\forall t\in T\\\left|P_{j,t}^{\mathrm{CHP}}-P_{j,t-1}^{\mathrm{CHP}}\right|\le\Delta P_j^{\mathrm{CHP}},&\forall i\in\Omega^{\mathrm{CHP}},\forall t\in T\end{cases}\tag{4}$$

where $P_i^{\mathrm{min/max}}$ and $P_j^{\mathrm{min/max}}$ are the minimum/maximum power generation of CFP unit *i* and CHP unit *j*, respectively. Constants $\Delta P_i^{\mathrm{CFP}}$ and $\Delta P_j^{\mathrm{CHP}}$ represent the ramping limit of CFP unit *i* and CHP unit *j* respectively. Additionally, at time *t*, the amount of on-grid wind power and unserved electricity should be lower than or equal to the actual wind power output ($P_{f,t}^{\mathrm{WA}}$) and the power load, respectively.

$$0\le P_{f,t}^{\mathrm{W}}\le P_{f,t}^{\mathrm{WA}},\quad\forall f\in\Omega^{\mathrm{WF}},\forall t\in T\tag{6}$$

$$0\le P_{e,t}^{\mathrm{UE}}\le P_{e,t}^{\mathrm{L}},\quad\forall e\in\Omega^{\mathrm{PL}},\forall t\in T\tag{7}$$

2) Optimal operation of the NGS

In the multi-energy model, the NGS aims at maximizing its social welfare, which is equal to the total

revenue of selling gas minus the total operational cost. The negative social welfare is minimized below.

$$\begin{aligned} f_{\mathrm{G}}(x) = \min_{\boldsymbol{x}^{\mathrm{NGS}}} \sum_{t\in T} \Bigg\{ & \sum_{k\in\Omega^{\mathrm{P2G}}} \left(fp_t^{\mathrm{ele}} P_{k,t}^{\mathrm{P2G}} \right) + \sum_{g\in\Omega^{\mathrm{S}}} C_g^{\mathrm{S}} G_{g,t}^{\mathrm{S}} \\ & + \sum_{s\in\Omega^{\mathrm{GS}}} \left(C_s^{\mathrm{GS,in}} G_{s,t}^{\mathrm{GS,in}} + C_s^{\mathrm{GS,out}} G_{s,t}^{\mathrm{GS,out}} \right) \\ & - \sum_{j\in\Omega^{\mathrm{CHP}}} fp_t^{\mathrm{gas}} G_{j,t}^{\mathrm{CHP}} - \sum_{g\in\Omega^{\mathrm{GL}}} u_{g,t}^{\mathrm{GL}} G_{g,t}^{\mathrm{L}} \Bigg\} \end{aligned} \tag{8}$$

where $\boldsymbol{x}^{\mathrm{NGS}}$ identifies the set of decision variables of the NGS. Constants C_g^{S} and $C_s^{\mathrm{GS,in/out}}$ are the marginal cost of gas generation from gas source *g* and the marginal cost of gas input/output of gas storage *s*, respectively. Variable fp_t^{gas} represents the hourly natural gas price. $G_{g,t}^{\mathrm{L}}$ is the hourly gas load at node *g* and variable $G_{j,t}^{\mathrm{CHP}}$ is the hourly gas consumption of CHP unit *j*. Variables $G_{g,t}^{\mathrm{S}}$ and $G_{s,t}^{\mathrm{GS,in/out}}$ represent the hourly gas generation of gas source *g* and hourly gas injection/extraction in/from the gas storage *s*, respectively. Thus, the objective function in the NGS optimization includes five components: the cost of P2G units to produce gas, the operational cost of gas supply from gas sources, operational cost of gas injection/extraction in/from the gas storages, the revenue from selling gas to gas-fired CHP units and the total utility for gas consumers, which is calculated by multiplying the amount of gas loads and the marginal utility of gas consumption ($u_{g,t}^{\mathrm{GL}}$).

For the gas network, the nodal gas balance is expressed as:

$$\begin{aligned} & \sum_{g\in\Omega^{\mathrm{S}}} G_{g,t}^{\mathrm{S}} + \sum_{s\in\Omega^{\mathrm{GS}}} \left(G_{s,t}^{\mathrm{GS,out}} - G_{s,t}^{\mathrm{GS,in}} \right) + \sum_{k\in\Omega^{\mathrm{P2G}}} G_{k,t}^{\mathrm{P2G}} \\ & + \sum_{l\in\Omega^{\mathrm{LP}}} \left(G_{l,t}^{\mathrm{LP,out}} - G_{l,t}^{\mathrm{LP,in}} \right) - \sum_{g\in\Omega^{\mathrm{GL}}} G_{g,t}^{\mathrm{L}} - \sum_{c\in\Omega^{\mathrm{GC}}} G_{c,t}^{\mathrm{GCC}} \\ & - \sum_{j\in\Omega^{\mathrm{CHP}}} G_{j,t}^{\mathrm{CHP}} = \sum_{n\in\Lambda_m} G_{mn,t}, \quad \forall m,n\in\Lambda^{\mathrm{NGS}}, \forall t\in T \end{aligned} \tag{9}$$

where variables $G_{k,t}^{\mathrm{P2G}}$ and $G_{c,t}^{\mathrm{GCC}}$ represent the hourly gas generation of P2G unit *k* and hourly gas consumption of gas compressor *c*, respectively. Variable $G_{l,t}^{\mathrm{LP,in/out}}$ is the gas linpack input/output in pipeline *l*. The hourly gas flow in pipeline *m*-*n* ($G_{mn,t}$) is determined by the pipeline resistance coefficient (Z_{mn}) and

the difference between the squared value of gas pressure at node m ($\pi_{m,t}$) and node n ($\pi_{n,t}$).

$$\pi_{m,t}-\pi_{n,t}=Z_{mn}\left(G_{mn,t}\right)^2,\quad \forall m,n\in\Lambda^{\mathrm{NGS}},\forall t\in T \tag{10}$$

The gas pressure of each node and the gas flow of each pipeline are subject to the pressure lower /upper limits ($\pi_{n,t}^{\min/\max}$) and the pipeline flow bounds (G_{mn}^{GP}), respectively.

$$\pi_{n,t}^{\min}\le\pi_{n,t}\le\pi_{n,t}^{\max},\quad \forall n\in\Lambda^{\mathrm{NGS}},\forall t\in T \tag{11}$$

$$\left|G_{mn,t}\right|\le G_{mn}^{\mathrm{GP}},\quad \forall m,n\in\Lambda^{\mathrm{NGS}},\forall t\in T \tag{12}$$

For each gas source, the gas production should be within its operational limits.

$$G_g^{\mathrm{S,min}}\le G_{g,t}^{\mathrm{S}}\le G_g^{\mathrm{S,max}},\quad \forall g\in\Omega^{\mathrm{S}},\forall t\in T \tag{13}$$

where $G_g^{\mathrm{S,min/max}}$ is the minimum/maximum gas generation of gas source g. Since the main component of natural gas is methane, the target product of P2G units in this paper is methane [10]. The relationship between gas consumption and power generation is expressed as:

$$G_{k,t}^{\mathrm{P2G}}=\eta_k^{\mathrm{P2G}}P_{k,t}^{\mathrm{P2G}},\quad \forall k\in\Omega^{\mathrm{P2G}},\forall t\in T \tag{14}$$

where constant η_k^{P2G} is the energy conversion efficiency of P2G unit k. The gas production of each P2G unit should be within its operational limits.

$$G_k^{\mathrm{P2G,min}}\le G_{k,t}^{\mathrm{P2G}}\le G_k^{\mathrm{P2G,max}},\quad \forall k\in\Omega^{\mathrm{P2G}},\forall t\in T \tag{15}$$

where $G_k^{\mathrm{P2G,min/max}}$ is the minimum/maximum gas generation of P2G unit k. Note that, gas compressors (GCs) can increase or maintain the pressure of the gas network by consuming gas or electricity. The hourly energy consumption in GC c is determined by its hourly gas flow rate ($G_{c,t}^{\mathrm{GC}}$) and its compression ratio (CR).

$$G_{c,t}^{\mathrm{GCC}}=\lambda_c^{\mathrm{GC}}G_{c,t}^{\mathrm{GC}},\quad \forall c\in\Omega^{\mathrm{GC}},\forall t\in T \tag{16}$$

where λ_c^{GC} is an operational parameter given by Eq. (17). For simplicity, all GCs are assumed to work at a constant compression ratio.

$$\lambda_g^{\mathrm{GC}}=K^{\mathrm{GC}}Z_{\mathrm{a}}\left[\frac{T_s}{E^{\mathrm{GC}}\eta^{\mathrm{GC}}}\right]\left[\frac{c_k}{c_k-1}\right]\left[(CR)^{\frac{c_k-1}{c_k}}-1\right] \tag{17}$$

where K^{GC} is the constant of GC g.

For gas storages, the mathematical model includes five components: gas injection limits, gas extraction limits, temporal energy balance, capacity limits and storage restoration.

$$\begin{cases} 0 \le G_{s,t}^{\mathrm{GS,in}} \le G_{s}^{\mathrm{GS,in,max}} \\ 0 \le G_{s,t}^{\mathrm{GS,out}} \le G_{s}^{\mathrm{GS,out,max}} \\ GS_{s,t} = GS_{s,0} + \sum_{t=1}^{T}\left(G_{s,t}^{\mathrm{GS,in}} - G_{s,t}^{\mathrm{GS,out}}\right) \quad \forall s \in \Omega^{\mathrm{GS}}, \forall t \in T \\ 0 \le GS_{s,t} \le GS_{s}^{\max} \\ GS_{s,T} = GS_{s,0} \end{cases} \tag{18}$$

where $G_{s}^{\mathrm{GC,in/out,max}}$ is the maximum gas input/output of gas storage s. Variable $GS_{s,t}$ represents the hourly gas stock in gas storage s. Constant $GS_{s}^{\max}$ is the capacity of gas storage s.

As an important component in balancing the gas production and consumption, the linepack refers to the amount of gas within a pipeline. Such amount of gas can vary within an acceptable range, and this ability is generally called linepack storage. Similar to gas storages, the mathematical model of linepacks can be expressed by the accumulated difference between the injection and extraction of gas in the pipeline.

$$\begin{cases} 0 \le LP_{l,t} \le LP_{l}^{\max} \\ LP_{l,t} = LP_{l,0} + \sum_{t=1}^{T}\left(G_{l,t}^{\mathrm{LP,in}} - G_{l,t}^{\mathrm{LP,out}}\right) \quad \forall l \in \Omega^{\mathrm{LP}}, \forall t \in T \\ LP_{l,T} = LP_{l,0} \end{cases} \tag{19}$$

where $LP_{l}^{\max}$ is the maximum gas stock in pipeline l. Variable $LP_{l,t}$ represents the hourly gas stock in pipeline l. Eq. (19) includes three components: linepack capacity limits, temporal energy balance and linepack restoration.

3) Optimal operation of the DHS

The DHS is a double-pipeline network including supply and return pipelines. The negative social welfare is minimized below.

$$
\begin{aligned}
f_{\mathrm{H}}(x) = \min_{\boldsymbol{x}^{\mathrm{DHS}}} \sum_{t\in T} \Bigg\{ & \sum_{j\in\Omega^{\mathrm{CHP}}} fp_t^{\mathrm{gas}} G_{j,t}^{\mathrm{CHP}} + \sum_{p\in\Omega^{\mathrm{HP}}} fp_t^{\mathrm{ele}} P_{p,t}^{\mathrm{HP}} \\
& + \sum_{s\in\Omega^{\mathrm{HS}}} \left(C_s^{\mathrm{HS,in}} H_{s,t}^{\mathrm{HS,in}} + C_s^{\mathrm{HS,out}} H_{s,t}^{\mathrm{HS,out}} \right) \\
& - \sum_{j\in\Omega^{\mathrm{CHP}}} fp_t^{\mathrm{ele}} P_{j,t}^{\mathrm{CHP}} - \sum_{h\in\Omega^{\mathrm{HL}}} u_{h,t}^{\mathrm{HL}} H_{h,t}^{\mathrm{L}} \Bigg\}
\end{aligned} \tag{20}
$$

where $\boldsymbol{x}^{\mathrm{DHS}}$ identifies the set of decision variables of the DHS. Constant $C_s^{\mathrm{HS,in/out}}$ is the marginal cost of heat input/output of heat storage *s*. Variable $H_{s,t}^{\mathrm{HS,in/out}}$ represents the hourly heat injection/extraction in/from heat storage *s*. $H_{h,t}^{\mathrm{L}}$ is the hourly heat load at node *h*. Thus, the objective function in the DHS optimization includes five components: the fuel cost of CHP units (or the cost of buying natural gas from the NGS), the operational cost of HPs (or the cost of buying electricity from the EPS), the operational cost of heat injections/extractions in/from heat storages, the revenue of selling electricity from CHP units to the EPS and the total utility for heat consumers, which is calculated by multiplying the amount of heat loads and the marginal utility of heat consumption ($u_{h,t}^{\mathrm{HL}}$).

For the heat network, the double constraint of nodal heat balance is expressed as:

$$
\begin{aligned}
& \sum_{j\in\Omega^{\mathrm{CHP}}} H_{j,t}^{\mathrm{CHP}} + \sum_{s\in\Omega^{\mathrm{HS}}} \left(H_{s,t}^{\mathrm{HS,out}} - H_{s,t}^{\mathrm{HS,in}} \right) + \sum_{p\in\Omega^{\mathrm{HP}}} H_{p,t}^{\mathrm{HP}} \\
& - \sum_{h\in\Omega^{\mathrm{HL}}} H_{h,t}^{\mathrm{L}} = c \cdot m_{mn,t} \cdot \left(\tau_{mn,t}^{\mathrm{out}} - \tau_{mn,t}^{\mathrm{in}} \right), \quad \forall m,n \in \Lambda^{\mathrm{DHS}}, \forall t \in T
\end{aligned} \tag{21}
$$

where variables $H_{j,t}^{\mathrm{CHP}}$ and $H_{p,t}^{\mathrm{HP}}$ represent the hourly heat generation of CHP unit *j* and HP *p*, respectively. Constant *c* is the specific heat capacity of water, variable $m_{mn,t}$ is the hourly mass flow rate of water in pipeline *m*-*n*, and variable $\tau_{mn,t}^{\mathrm{in/out}}$ is the hourly temperature at the inlet/outlet of pipeline *m*-*n*. In order to consider heat losses in the DHS, the temperature drop along the water pipeline *m*-*n* is described as:

$$
\tau_{mn,t}^{\mathrm{out}} - \tau_{mn,t}^{\mathrm{am}} = \lambda_{mn,t} \left(\tau_{mn,t}^{\mathrm{in}} - \tau_{mn,t}^{\mathrm{am}} \right), \quad \forall m,n \in \Lambda^{\mathrm{DHS}}, \forall t \in T \tag{22}
$$

where constant $\tau_{mn,t}^{\mathrm{am}}$ is the hourly ambient temperature, and constant $\lambda_{mn,t}$ is the temperature drop coefficient of water pipeline *m*-*n* given as:

$$\lambda_{mn,t} = \exp\left(-\frac{k_{mn}\pi d_{mn} l_{mn}}{c \cdot m_{mn,t}}\right) \tag{23}$$

To ensure that the DHS optimization problem is linear, the DHS is assumed to work under a control strategy of constant water-flow and variable-temperature. Hence, the mass flow rate of water ($m_{mn,t}$) is constant and the coefficient $\lambda_{mn,t}$, which is determined by pipeline parameters and $m_{mn,t}$, is also constant. In other words, these two important parameters are chosen according to the operating specifications of the different heat networks. For each supply/return pipeline, the hourly temperature of pipeline *m*-*n* ($\tau_{mn,t}$) should be within the setting range of the DHS.

$$\tau_{mn}^{\min} \le \tau_{mn,t} \le \tau_{mn}^{\max}, \qquad \forall m,n \in \Lambda^{\mathrm{DHS}}, \forall t \in T \tag{24}$$

where $\tau_{mn}^{\min/\max}$ is the minimum/maximum temperature of heating pipeline *m*-*n*. Based on mass conservation, the nodal temperature of mixed water and nodal mass flow balance are respectively expressed as:

$$\tau_{n,t} \sum_{m \in \Lambda_n} m_{mn,t} = \sum_{m \in \Lambda_n} \left(m_{mn,t} \cdot \tau_{mn,t}^{\mathrm{out}}\right), \qquad \forall m,n \in \Lambda^{\mathrm{DHS}}, \forall t \in T \tag{25}$$

$$\sum_{m \in \Lambda_n} m_{mn,t} = 0, \qquad \forall m,n \in \Lambda^{\mathrm{DHS}}, \forall t \in T \tag{26}$$

For each CHP unit, the conversion relationship among the gas consumption, electricity and heat production is expressed as:

$$H_{j,t}^{\mathrm{CHP}} = P_{j,t}^{\mathrm{CHP}} \cdot \left[\left(1-\eta_j^{\mathrm{e}}-\eta_j^{\mathrm{LOSS}}\right) \cdot K_j^{\mathrm{e}}\right] \Big/ \eta_j^{\mathrm{e}}, \qquad \forall j \in \Omega^{\mathrm{CHP}}, \forall t \in T \tag{27}$$

$$P_{j,t}^{\mathrm{CHP}} = \eta_j^{\mathrm{e}} G_{j,t}^{\mathrm{CHP}}, \qquad \forall j \in \Omega^{\mathrm{CHP}}, \forall t \in T \tag{28}$$

where constants η_j^{e}, η_j^{LOSS} and K_j^{e} represent the electricity production efficiency, heat loss coefficient and heat exchange coefficient of CHP unit *j*, respectively. Since this paper only considers back-pressure CHP units, a constant parameter, heat-power ratio (r_j^{htp}), is introduced to describe the relationship between the production of heat and power of each CHP unit, where $r_j^{\mathrm{htp}} = \left[\left(1-\eta_j^{\mathrm{e}}-\eta_j^{\mathrm{LOSS}}\right) \cdot K_j^{\mathrm{e}}\right] \Big/ \eta_j^{\mathrm{e}}$.

As more effective heat generators than electrical resistance heaters, HPs are widely used for heating

purposes [26]. For each HP, the relationship between heat generation and electricity consumption is defined as:

$$H_{p,t}^{\mathrm{HP}} = COP \cdot P_{p,t}^{\mathrm{HP}}, \quad \forall p \in \Omega^{\mathrm{HP}}, \forall t \in T \tag{29}$$

where *COP* is the coefficient of performance of the HP. Additionally, the electricity production of each HP should be within its operational limits.

$$H_{p}^{\mathrm{HP,min}} \le H_{p,t}^{\mathrm{HP}} \le H_{p}^{\mathrm{HP,max}}, \quad \forall p \in \Omega^{\mathrm{HP}}, \forall t \in T \tag{30}$$

where $H_p^{\mathrm{HP,min/max}}$ is the minimum/maximum heat generation of HP *p*. For the heat storages, the mathematical model includes five components: heat input limits, heat output limits, temporal energy balance, capacity limits and storage restoration.

$$\begin{cases} 0 \le H_{s,t}^{\mathrm{HS,in}} \le H_{s}^{\mathrm{HS,in,max}} \\ 0 \le H_{s,t}^{\mathrm{HS,out}} \le H_{s}^{\mathrm{HS,out,max}} \\ HS_{s,t+1} = HS_{s,t} + \left(H_{s,t}^{\mathrm{HS,in}} - H_{s,t}^{\mathrm{HS,out}} \right) \quad \forall s \in \Omega^{\mathrm{HS}}, \forall t \in T \\ 0 \le HS_{s,t} \le HS_{s}^{\max} \\ HS_{s,T} = HS_{s,0} \end{cases} \tag{31}$$

where $H_s^{\mathrm{HS,in/out,max}}$ is the maximum gas input/output of heat storage *s*. Variable $HS_{s,t}$ represents the hourly heat stock in heat storage *s*. Constant $HS_s^{\max}$ is the capacity of heat storage *s*.

As we described above, the equilibrium problem is summarized as follows.

$$\begin{aligned} &\text{Find}\left(\boldsymbol{x}^{\mathrm{EPS}}, \boldsymbol{x}^{\mathrm{NGS}}, \boldsymbol{x}^{\mathrm{DHS}}, \boldsymbol{fp} \right) \text{satisfying, } \boldsymbol{fp} = \left\{ fp_t^{\mathrm{gas}}, fp_t^{\mathrm{ele}} \right\} \\ &f_{\mathrm{E}}(x) = \min_{\boldsymbol{x}^{\mathrm{EPS}}}, \quad \boldsymbol{x}^{\mathrm{EPS}} = \left\{ P_{i,t}^{\mathrm{CFP}}, P_{f,t}^{\mathrm{W}}, P_{j,t}^{\mathrm{CHP}}, P_{e,t}^{\mathrm{UE}}, \delta_{n,t} \right\} \\ &\text{s.t.} \quad \begin{cases} \text{Linking constraints } (14), (27)-(29) \\ \text{EPS constraints } (2)-(7) \end{cases} \\ &f_{\mathrm{G}}(x) = \min_{\boldsymbol{x}^{\mathrm{NGS}}}, \quad \boldsymbol{x}^{\mathrm{NGS}} = \left\{ G_{g,t}^{\mathrm{S}}, G_{k,t}^{\mathrm{P2G}}, G_{s,t}^{\mathrm{GS,in/out}}, G_{s,t}^{\mathrm{LP,in/out}}, \pi_{n,t} \right\} \\ &\text{s.t.} \quad \begin{cases} \text{Linking constraints } (14), (27)-(29) \\ \text{EPS constraints } (9)-(13), (15)-(19) \end{cases} \\ &f_{\mathrm{H}}(x) = \min_{\boldsymbol{x}^{\mathrm{DHS}}}, \quad \boldsymbol{x}^{\mathrm{DHS}} = \left\{ H_{j,t}^{\mathrm{CHP}}, H_{p,t}^{\mathrm{HP}}, H_{s,t}^{\mathrm{HS,in/out}}, \tau_{mn,t}^{\mathrm{in/out}} \right\} \\ &\text{s.t.} \quad \begin{cases} \text{Linking constraints } (14), (27)-(29) \\ \text{EPS constraints } (21)-(26), (30)-(31) \end{cases} \end{aligned} \tag{32}$$

As shown in Fig. 1, the connection variables among different subsystems are $G_{j,t}^{\mathrm{CHP}}$, $P_{j,t}^{\mathrm{CHP}}$, $P_{p,t}^{\mathrm{HP}}$ and $P_{k,t}^{\mathrm{P2G}}$. These variables are determined by the energy conversion relationships of P2G units (14), CHP units (27), (28) and HPs (29), respectively. For each subsystem problem, both the linking constraints and its operational constraints should be satisfied. This fact makes all subsystem problems interdependent and results in an equilibrium problem. Although the decision variables of each subsystem problem ($\boldsymbol{x}^{\mathrm{EPS}}$, $\boldsymbol{x}^{\mathrm{NGS}}$, $\boldsymbol{x}^{\mathrm{DHS}}$) are just those in the subsystem optimization vector, the objective function, the constraints and the decision of each problem depend on the decision variables of all the problems. In other words, an equilibrium must simultaneously optimize all subsystems' objectives and constraints [15]. Furthermore, the market prices ($fp_t^{\mathrm{gas}}, fp_t^{\mathrm{ele}}$) depend on all subsystems' decisions and are obtained by solving the corresponding equilibrium problem.

2.3 Centralized optimization model

For the sake of comparison, we also consider a MES controlled by a central entity that jointly operate the NES, the NGS and the DHS to maximize social welfare, which refers to the cost of energy production minus the utility of energy consumption. Here, the objective function of the centralized model is given by Eq. (33). It has six components including the operational cost of CFP units, the cost of gas supply from gas sources, the operational cost of gas injection/extraction in/from gas storages, the operational cost of heat injection/extraction in/from heat storages, the utility of electricity consumption, the utility of gas consumption and the utility of heat consumption. The operational cost is considered to be zero for wind power. The centralized model is:

$$\begin{aligned} f\left(\boldsymbol{x}\right) = \min \sum_{t\in T} \Bigg\{ & \sum_{i\in\Omega^{\mathrm{CFP}}} C_i^{\mathrm{CFP}} P_{i,t}^{\mathrm{CFP}} + \sum_{g\in\Omega^{\mathrm{GS}}} C_g^{\mathrm{S}} G_{g,t}^{\mathrm{S}} + \sum_{s\in\Omega^{\mathrm{GS}}} \left(C_s^{\mathrm{GS,in}} Q_{s,t}^{\mathrm{GS,in}} + C_s^{\mathrm{GS,out}} Q_{s,t}^{\mathrm{GS,out}} \right) \\ & + \sum_{s\in\Omega^{\mathrm{HS}}} \left(C_s^{\mathrm{HS,in}} H_{s,t}^{\mathrm{HS,in}} + C_s^{\mathrm{HS,out}} H_{s,t}^{\mathrm{HS,out}} \right) - \sum_{e\in\Omega^{\mathrm{PL}}} u_{e,t}^{\mathrm{PL}} P_{e,t}^{\mathrm{L}} - \sum_{g\in\Omega^{\mathrm{GL}}} u_{g,t}^{\mathrm{GL}} G_{g,t}^{\mathrm{L}} - \sum_{h\in\Omega^{\mathrm{HL}}} u_{h,t}^{\mathrm{HL}} H_{h,t}^{\mathrm{L}} \Bigg\} \end{aligned} \tag{33}$$

$$\boldsymbol{x} = \left\{ \boldsymbol{x}^{\mathrm{EPS}}, \boldsymbol{x}^{\mathrm{NGS}}, \boldsymbol{x}^{\mathrm{DHS}} \right\}$$

subject to:

operational constraints of the EPS (2)-(7),

operational constraints of the NGS (9)-(19), and

operational constraints of the DHS (21)-(31).

It is worth mentioning that, for each gas-fired CHP unit, the fuel cost is calculated as a part of the cost of gas supply in the NGS system and is not specified in the objective function. Similarly, for the HPs and P2G units, there are no fuel costs in their operational costs, as the fuel costs are computed as a part of the cost of electricity supply in the EPS. The optimization is subject to all constraints, including energy conversion relationships, electric power constraints, natural gas constraints, and district heating constraints.

3. SOLUTION METHODOLOGY

The equilibrium problem is defined by simultaneously considering the optimization problems of the three subsystems as shown in Fig. 2. The equilibrium problem is defined by simultaneously considering the optimization problems of the three subsystems as shown in Fig. 2. It shows that each optimization problem includes an objective function, equality constraints and inequality constraints. KKT conditions are necessary conditions for optimality. For a linear and convex optimization problem, KKT conditions are both necessary and sufficient [29], which means that the whole problem can be replaced with the corresponding KKT conditions.

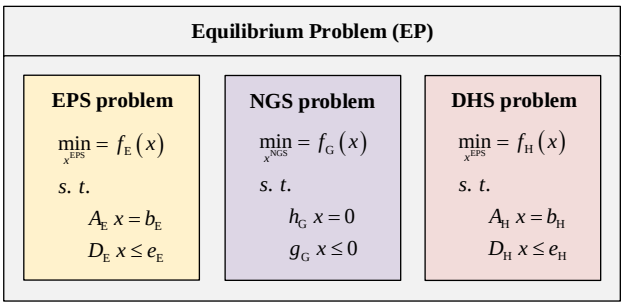

Fig. 2. Equilibrium problem: joint solution of the interrelated optimization problems of the EPS, the NGS and the DHS

In the optimization problems of the EPS and the DHS, the objective functions are linear and are subject to linear constraints. It means that the optimization problems of these two subsystems are linear. Therefore, the

KKT conditions of these subsystem problems are both necessary and sufficient. However, for the optimization problem of the NGS, the objective function is linear while the constraints contain a non-convex Eq. (10). In a normal operating situation, the gas supplied by the gas source and the gas stored in the gas storage exhibit a rather flat profile due to the capacity of linepack storages. If the variation of the gas content in the pipeline is restricted within a narrow limit, Eq. (10) can be rewritten as a convex equation as shown in reference [7]. The resulting NGS problem is also convex. The corresponding equilibrium problem is obtained by jointly solving the KKT conditions of the three convex problems as shown in Fig. 3. PATH is used to solve this equilibrium problem [23].

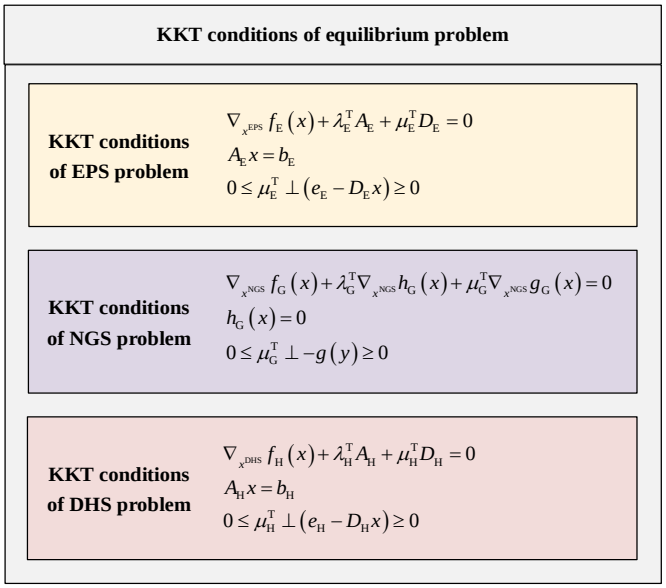

Fig. 3. KKT conditions of equilibrium problem: joint solution of the EPS, the NGS and the DHS

4. CASE STUDY

4.1 Description of the simulation system

In this section, the proposed model is applied to a MES, which consists of a 4-bus electricity system, a 4-node gas system and a 6-node heat system. The topology of this test system is shown in Fig. 4. The gas network is composed of four nodes, three pipelines, one gas storage and one gas compressor. The 4-bus electricity system includes a CFP unit, a CHP unit and a wind farm. The heat system has one heat storage and six nodes. There are three coupling points among the gas, heat and electricity systems: the CHP unit, the

P2G unit and the HP. The detailed parameters for the units and network topologies are given in Tab. 1, including the gas well, the gas linepack, the heat storage, the gas storage, the CFP unit, the CHP unit and the P2G unit. Additional data obtained from Energinet.dk [28] (the transmission system operator for electricity and natural gas in Denmark) is provided in Tab. 2. These data include the gas demand, the electricity demand and the wind power production. The heat demand is set based on reference [9]. It should be mentioned that the data have been scaled to fit this case study.

For a time horizon of 24 hours, the equilibrium problem includes 1038 positive variables, 456 free variables, 1416 inequality constraints, and 676 equality constraints. Since this problem is a nonlinear complementarity problem, it is solved using PATH under GAMS [29]. The centralized optimization problem is a nonlinear programming problem, which is solved using IPOPT under GAMS. Since the performance of the solver depends on the initial solution, a number of starting points are randomly generated within appropriate limits by using the heuristic rule. The laptop used has an Intel (R) Core (TM) i7 CPU clocking at 2.70 GHz and 8 GB of RAM. The computational time for each simulation is less than 10 seconds. For this test system, computation times are small and acceptable for operational requirements. Considering larger systems will raise computational challenges. However, cloud computing and parallel algorithms can be used to achieve tractability.

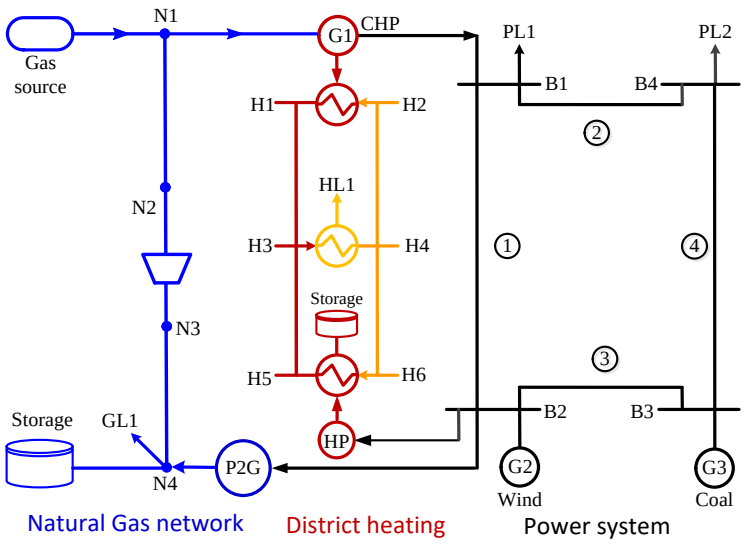

Fig. 4. The structure of an integrated electricity, gas and district heating system

Table 1 Data of The detailed parameters for the units and network

Parameter	Value	Unit
C_i^{CFP}	15	€/MWh
C_g^{S}	12	
$C_s^{\mathrm{GS,in/out}}$	2/14	
$C_s^{\mathrm{HS,in/out}}$	2/10	
$\sigma_{e,t}^{\mathrm{UE}}$	35	
$u_{e,t}^{\mathrm{PL}}$	18	
$u_{g,t}^{\mathrm{GL}}$	16	
$u_{h,t}^{\mathrm{HL}}$	14	
$P_i^{\mathrm{min/max}}$	50/270	MW
$\Delta P_i^{\mathrm{CFP}}$	60	
$P_j^{\mathrm{min/max}}$	0/45	
$\Delta P_j^{\mathrm{CHP}}$	25	
$G_g^{\mathrm{S,min/max}}$	90/235	
$H_p^{\mathrm{HP,min/max}}$	0/60	
$G_k^{\mathrm{P2G,min/max}}$	0/15	
$G_s^{\mathrm{GS,in/out,max}}$	50/50	
$H_s^{\mathrm{HS,in/out,max}}$	5/5	
P_{mn}^{TL}	500	
G_{mn}^{GP}	500	
$GS_s^{\max}$	300	MWh
$HS_s^{\max}$	80	
$LP_l^{\max}$	90	
λ_c^{GC}	99	%
η_k^{P2G}	40	
COP	200	
η_j^{e}	30	
r_j^{htp}	$\frac{5}{3}$	-

Table 2 Data of the output of wind power and multi-energy demand in the time horizon [MW]

Time	1	2	3	4	5	6	7	8	9	10	11	12
LWP	85.5	65.7	51.8	41.1	28.8	23.5	26.8	18.8	13.2	12.5	7.9	7.2
HWP	172.0	185.0	180.0	200.0	209.0	215.5	211.8	206.0	200.0	187.0	179.0	172.0
ED	179.6	176.8	175.3	177.8	194.0	238.2	289.0	306.0	304.6	309.6	308.8	301.2
GD	130.0	131.0	137.5	147.2	165.5	178.9	183.2	187.7	188.6	188.1	185.0	183.3
HD	50.0	50.0	48.6	49.0	49.0	49.0	48.0	47.0	46.0	44.5	43.5	43.0

Time	13	14	15	16	17	18	19	20	21	22	23	24
LWP	8.0	13.8	18.8	25.0	26.8	32.9	38.0	41.4	40.1	47.9	60.2	80.1
HWP	166.0	164.0	165.0	168.0	173.0	179.0	201.0	212.5	219.0	225.0	230.0	225.0
ED	303.6	300.1	293.1	306.3	327.0	308.6	287.2	267.3	248.5	227.2	206.6	193.5
GD	180.5	184.6	189.6	193.4	192.6	187.7	168.1	150.7	135.0	130.2	126.9	126.2
HD	42.5	42.5	43.0	43.0	43.5	44.5	45.0	45.0	45.5	46.4	46.8	47.2

LWP: low-wind power; HWP: high-wind power;
GD: gas demand; ED: electricity demand; HD: heat demand

4.2 Equilibrium and centralized optimization

The model considered in this paper results in a Generalized Nash Equilibrium Problem (GNEP), which is a generalization of the well-known Nash Equilibrium Problem in which each player's strategy depends on the actions of the other players [15], [29]. Simulation results are summarized in Tab. 3. The results show that all cases converge to a single equilibrium, whose cost and social welfare are those of the centralized optimization problem. For the centralized optimization problem, perfect coordination among the three operators is assumed. For the equilibrium problem, all subsystems are considered as price takers. The results show that if perfect information coordination among the subsystems exists, the Nash equilibria is a globally optimal solution in spite of each subsystem focusing on maximizing its own social welfare.

From the perspective of optimization, the outcome of the equilibrium model is the same as that of the centralized model. However, the core significances of the equilibrium model and the centralized model are not the same from the perspective of markets. In the existing market conditions, perfect competition and monopoly exist at the same time. The operators of different energy systems may have their own internal information protection mechanisms and they are generally unwilling to share information (network parameters, real-time data, etc.) without reservation. Thus, the centralized model that has to rely on a central entity to collect information of all subsystems might not be appropriate for analyzing a multi-energy market in practice. For the equilibrium model, there is no need for a central operator and each subsystem operator can have its own objective that is subject to the operational constraints of its internal parameters. In the case of limited coordination between energy subsystems, the equilibrium model allows each subsystem operator to build its operation optimization in the internal system, forms a gaming problem between these subsystem optimizations, and then searches an equilibrium solution through limited coupling information. This equilibrium solution may not be a globally optimal solution, but it can enable subsystem operators to satisfy their respective interests while protecting their internal information. The equilibrium model can deal with the consequence of imperfect coordination or imperfect information exchange, analyze the market behavior of each subsystem and simulate the market interactions between the subsystems in a clear way. This is why the

equilibrium model is proposed.

Table 3 Results of equilibrium and centralized optimization

Type	Profit-NGS	Profit-EPS	Profit-DHS	Total SW	Total Cost
	$	$	$	$	$
CP	-	-	-	48187	142970
EP	14926	28579	4682	48187	142970

CP: Centralized problem; EP: equilibrium problem; SW: social welfare

4.3 Pricing and scheduling of the MES

Price information is one of the most important market outcomes. To further explore the interaction between the different subsystems, the daily variations of energy prices obtained from the equilibrium model are analyzed. To analyze the effect of different wind power profile on the market outcomes and energy exchanges, the equilibrium model is run under a low-wind scenario and a high wind scenario, as shown in Fig. 5. The simulation results are illustrated in Figs. 6-13, including market clearing prices, energy exchanges, electricity scheduling, gas scheduling and heat scheduling. It should be noted that the total gas consumption consists of the gas demand and the gas consumed by the gas compressor and the CHP unit; the total electricity consumption includes the electricity demand and the electricity consumed by the P2G unit and the HP; the total heat consumption involves the heat demand and the heat loss. The heat loss is mainly caused by the heat transfer from high-temperature water to the ambiance.

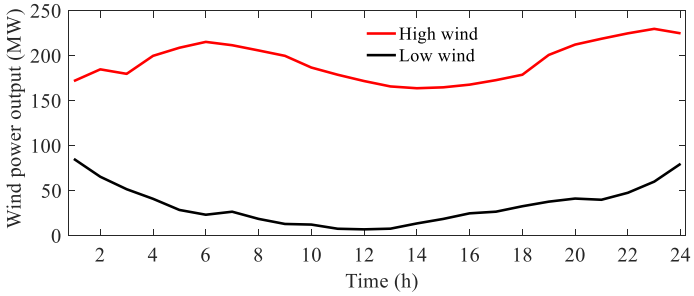

Fig. 5. Two scenarios of wind power output

The energy prices of gas and electricity are shown in Figs. 6 and Fig. 7 over a 24-hour horizon. Since there is no congestion and power losses are ignored, the electricity prices are the same at all nodes.

In the low-wind scenario, during the periods 1h-6h, the electricity price (15$/MWh) is the same as the

marginal cost of power generation from the CFP unit and the gas price (12$/MWh) is the same as the marginal cost of gas supply from the gas source (Fig. 6). The wind generation and the CFP unit supply the electricity demand (Fig. 8) and the gas source supply all gas demand. Since there is enough wind power in the MES and the electricity price is low, all the heat demand is supplied by the HP that has a high conversion efficiency (Fig. 10). Starting from period 7h, the electricity price increases to 21.9$/MWh and reaches its highest value with a load shedding of 0.6MWh in period 11h (Fig. 6). On the other hand, during period 7h-14h, the gas price increases to the marginal cost of gas output of the gas source (14$/MWh). The reason for this energy price change is that as the wind power output decreases and the power load increases, the CHP unit has better economic performance and starts supplying heat and power (Fig. 10). However, the operation of the CHP unit causes an increase of gas consumption in the NGS, which means that the gas storage needs to provide gas (Fig. 12). In Fig. 12, there is a difference between gas supply and consumption, which is offset by the gas linepack. It can be seen that the gas linepack is used during the day and restored at midnight. At 15h, the gas price decreases since all gas consumption are met by the gas source and the linepack, which leads to a decrease in the electricity price (Fig. 6). From period 16h to period 17h, the power demand reaches the peak load, and the gas storage operates again (Fig. 12), which result in an increase of the gas price and the electricity price. During the periods 18h-24h, the reduction of the gas and electricity demands leads to the decrease of the gas and electricity prices (Fig. 6). At the same time, with the increase of the wind power output, the heat production of the CHP is gradually reduced until the heat demand is fully satisfied by the HP (Fig. 12).

In the high-wind scenario, since the wind power is abundant, the heat demand is completely satisfied by the HP and the CHP is not used (Fig. 11). The gas price is consistent (12$/MWh) as shown in Fig. 7. During the valley load periods, 1h-5h and 22-24h, in the EPS, part of the surplus wind power is converted into heat and gas via the HP unit and the P2G unit, respectively (Fig. 11 and Fig. 13). Meanwhile, the electricity price is as low as 4.8 $/MWh as shown in Fig. 7. Specifically, in period 4h and period 23h, there is wind spillage and the electricity price is zero, the marginal cost of the wind power unit. During the periods 6h-21h, the

power consumption increases and is met by the CFP unit and the wind power unit (Fig. 9). The electricity price is around 18.05 $/MWh (Fig. 7). It is worth mentioning that there is still some wind curtailment in the periods 23h-24h due to the capacity of the P2G unit.

Tab. 4 compares the simulation results in terms of social welfare and total cost for the low-wind and high-wind scenarios. The social welfare goes up with the wind power output, while the total cost goes down. Higher wind output means that more electricity demand can be supplied from “free” wind power and more heat loads can be supplied by the HP with low electricity price. Further, surplus wind power can be converted to gas through the P2G unit, which reduces the gas supply cost from the gas storage. This results in higher profit and a lower total cost for the MES as a whole.

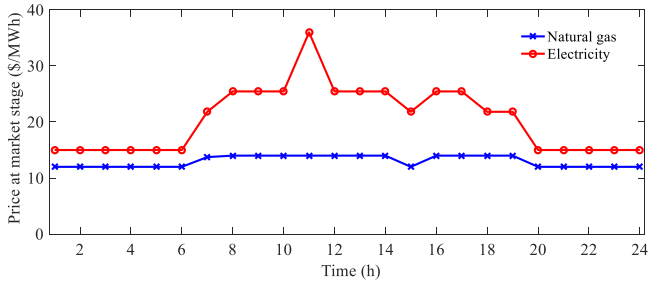

Fig. 6. Daily energy price variation under low-wind scenario

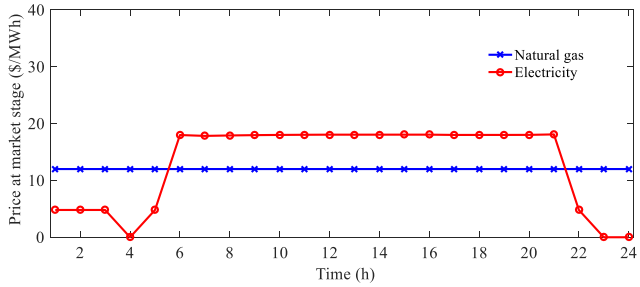

Fig. 7. Daily energy price variation under high-wind scenario

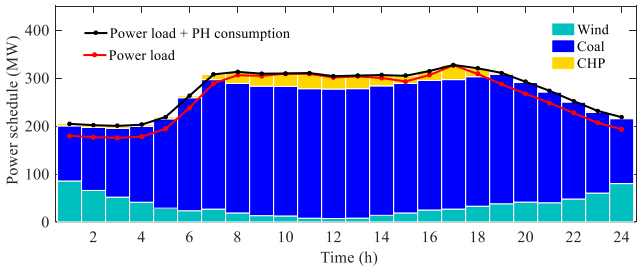

Fig. 8. Energy output in the EPS under low-wind scenario.

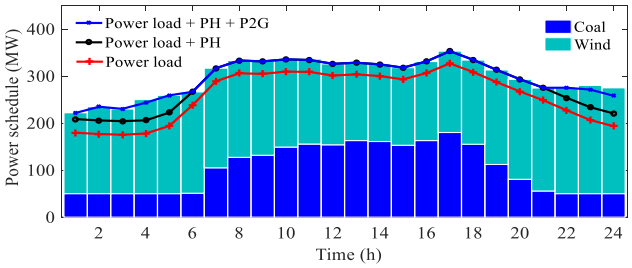

Fig. 9. Energy output in the EPS under high-wind scenario

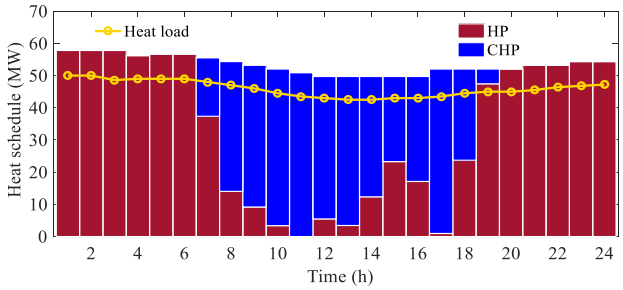

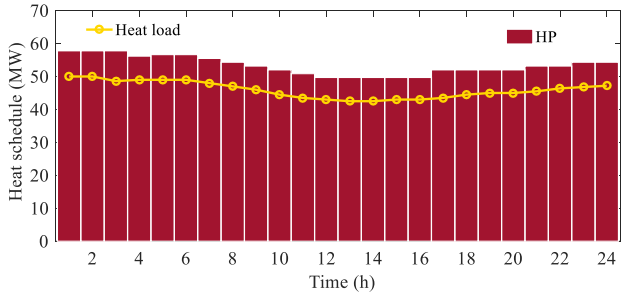

Fig. 10. Energy output in the DHS under low-wind scenario. Fig. 11. Energy output in the DHS under high-wind scenario.

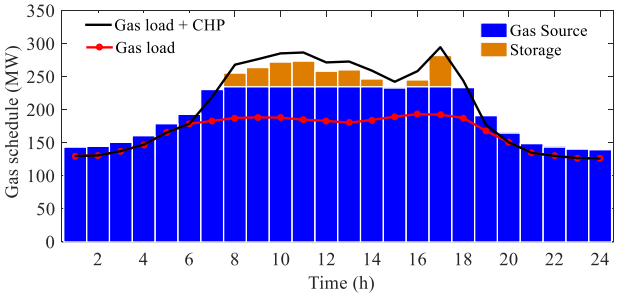

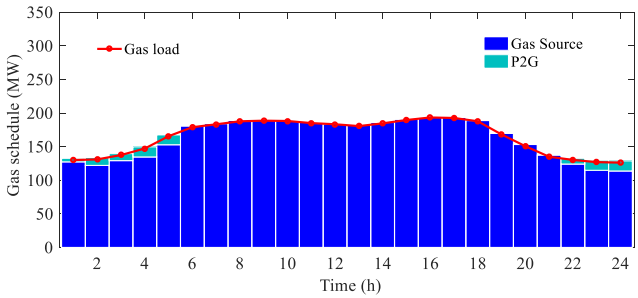

Fig. 12. Energy output in the NGS under low-wind scenario. Fig. 13. Energy output in the NGS under high-wind scenario

Table 4 Comparison of simulation results in two scenarios

Case	Profit-NGS	Profit-EPS	Profit-DHS	Total SW	Total Cost
	$	$	$	$	$
LW	14926	28579	4682	48187	142970
HW	15951	83453	7334	106738	84424

SW: social welfare; LW: low-wind; HW: high-wind

5. CONCLUSION

This paper proposes a model to characterize the coordinated operation of the electricity, gas and district heating systems in a district and urban area. An equilibrium model is developed to represent the interactions of the energy players in the MES. The equilibrium is identified by jointly solving the KKT conditions of the individual but interrelated energy optimization problems. The resulting equilibrium problem is a nonlinear complementarity problem and is solved using PATH. The proposed equilibrium model is compared with a centralized optimization model. The result of the equilibrium problem is the same as that of the centralized optimization problem if perfect coordination/communication among the three operators occurs. More importantly, the simulation results show that the proposed equilibrium model preserve the independence of each subsystem and allow analyzing the market interactions and the energy exchange among these subsystems. Future work will analyze the efficiency loss as a result of limited information interchange among the operation of the three energy subsystems.

ACKNOWLEDGMENTS

The EUDP Project ‘Sustainable Energy Market Integration (SEMI)’ supports this work (EUDP17-I: 12554) In addition, the authors gratefully acknowledge the support of China Scholarship Council. Partial support is also provided by LIS NSF grant 1808169.

REFERENCES

[1] P. Mancarella, “MES (multi-energy systems): An overview of concepts and evaluation models,” *Energy*, vol. 65, pp. 1–17, Feb. 2014.

[2] H. Lund, “Renewable heating strategies and their consequences for storage and grid infrastructures comparing a smart grid to a smart energy systems approach,” *Energy*, vol. 151, pp. 94–102, Mar. 2018.

[3] H. Lund, P. A. Østergaard, M. Chang, S. Werner et al., “The status of 4th generation district heating: Research and results,” *Energy*, vol. 164, pp. 147–159, Jun. 2018.

[4] H. Lund, P. A. Østergaard, D. Connolly and B. V. Mathiesen “Smart energy and smart energy systems,” *Energy*, vol. 137, pp. 556–565, Feb. 2017.

[5] D. Connolly, H. Lund, B. V. Mathiesen, S. Werner et al., “Heat Roadmap Europe: Combining district heating with heat savings to decarbonise the EU energy system,” *Energy Policy*, vol. 65, pp. 475–489, Feb. 2014.

[6] Q. Zeng, J. Fang, J. Li, and Z. Chen, “Steady-state analysis of the integrated natural gas and electric power system with bi-directional energy conversion,” *Appl. Energy*, vol. 184, pp. 1483–1492, Dec. 2016.

[7] J. Fang, Q. Zeng, X. Ai, Z. Chen, and J. Wen, “Dynamic Optimal Energy Flow in the Integrated Natural Gas and Electrical Power Systems,” *IEEE Trans. Sustain. Energy*, vol. 9, no. 1, pp. 188–198, Jan. 2018.

[8] X. Zhang, M. Shahidehpour, A. Alabdulwahab, and A. Abusorrah, “Hourly Electricity Demand Response in the Stochastic Day-Ahead Scheduling of Coordinated Electricity and Natural Gas Networks,” *IEEE Trans. Power Syst.*, vol. 31, no. 1, pp. 592–601, Jan. 2016.

[9] B. Zhao, A. J. Conejo, and R. Sioshansi, "Unit Commitment Under Gas-Supply Uncertainty and Gas-Price Variability," *IEEE Trans. Power Syst.*, vol. 32, no. 3, pp. 2394–2405, May 2017.

[10] C. Liu, C. Lee, and M. Shahidehpour, "Look Ahead Robust Scheduling of Wind-Thermal System With Considering Natural Gas Congestion," *IEEE Trans. Power Syst.*, vol. 30, no. 1, pp. 544–545, Jan. 2015.

[11] X. Liu, J. Wu, N. Jenkins, and A. Bagdanavicius, "Combined analysis of electricity and heat networks," *Appl. Energy*, vol. 162, pp. 1238–1250, Jan. 2016.

[12] J. Li, J. Fang, Q. Zeng, and Z. Chen, "Optimal operation of the integrated electrical and heating systems to accommodate the intermittent renewable sources," *Appl. Energy*, vol. 167, pp. 244–254, Apr. 2016.

[13] Z. Li, W. Wu, M. Shahidehpour, J. Wang, and B. Zhang, "Combined Heat and Power Dispatch Considering Pipeline Energy Storage of District Heating Network," *IEEE Trans. Sustain. Energy*, vol. 7, no. 1, pp. 12–22, Jan. 2016.

[14] Z. Li, W. Wu, J. Wang, B. Zhang, and T. Zheng, "Transmission-Constrained Unit Commitment Considering Combined Electricity and District Heating Networks," *IEEE Trans. Sustain. Energy*, vol. 7, no. 2, pp. 480–492, Apr. 2016.

[15] S. A. Gabriel, A. J. Conejo, J. D. Fuller, B. F. Hobbs, and C. Ruiz, *Complementarity Modeling in Energy Markets*, vol. 180. New York, NY: Springer New York, 2013.

[16] F. Facchinei and C. Kanzow, "Generalized Nash equilibrium problems," *4OR*, vol. 5, no. 3, pp. 173–210, Sep. 2007.

[17] C. Ruiz, A. J. Conejo, and R. García-Bertrand, "Some analytical results pertaining to Cournot models for short-term electricity markets," *Electr. Power Syst. Res.*, vol. 78, no. 10, pp. 1672–1678, Oct. 2008.

[18] B. F. Hobbs and U. Helman, "Complementarity-based equilibrium modeling for electric power markets," *Model. Prices Compet. Electr. Mark.*, 2004.

[19] B. F. Hobbs, C. B. Metzler, and J. S. Pang, "Strategic gaming analysis for electric power systems: an MPEC approach," *IEEE Trans. Power Syst.*, vol. 15, no. 2, pp. 638–645, May 2000.

[20] C. Ruiz, A. J. Conejo, J. D. Fuller, S. A. Gabriel, and B. F. Hobbs, "A tutorial review of complementarity models for decision-making in energy markets," *EURO J. Decis. Process.*, vol. 2, no. 1–2, pp. 91–120, Jun. 2014.

[21] D. Pozo and J. Contreras, "Finding Multiple Nash Equilibria in Pool-Based Markets: A Stochastic EPEC Approach," *IEEE Trans. Power Syst.*, vol. 26, no. 3, pp. 1744–1752, Aug. 2011.

[22] H. Yang, C. Y. Chung, and K. P. Wong, "Optimal Fuel, Power and Load-Based Emissions Trades for Electric Power Supply Chain Equilibrium," *IEEE Trans. Power Syst.*, vol. 27, no. 3, pp. 1147–1157, Aug. 2012.

[23] S. P. Dirkse and M. C. Ferris, "The PATH Solver: A Non-Monotone Stabilization Scheme for Mixed Complementarity Problems," *Optim. Methods Softw.*, vol. 5, pp. 123–156, 1995.

[24] M. J. Osborne and A. Rubinsterin, *A Course in Game Theory*, pp. 14. Cambridge, MA: MIT, 1994.

[25] J. M. Morales, A. J. Conejo, H. Madsen, P. Pinson, and M. Zugno, *Integrating Renewables in Electricity Markets*, vol. 205. Boston, MA: Springer US, 2014.

[26] K. J. Chua, S. K. Chou, and W. M. Yang, "Advances in heat pump systems: A review," *Appl. Energy*, vol. 87, no. 12, pp. 3611–3624, Dec. 2010.

[27] M. S. Bazaraa, H. D. Sherali, and C. M. Shetty, "The Fritz John and Karush–Kuhn–tucker Optimality Conditions," in *Nonlinear Programming*, John Wiley & Sons, Inc., 2006, pp. 163–236.

[28] Energinet.dk, "Download of market data." [Online]. Available: https://en.energinet.dk/. [Accessed: 12-Dec-2017].

[29] A. Brook, D. Kendrick, and A. Meeraus, "GAMS, a User's Guide," *SIGNUM Newsl*, vol. 23, no. 3–4, pp. 10–11, Dec. 1988.